Int. J. Multiphase Flow Vol. 15, No. 3, pp. 393–401, 1989
Printed in Great Britain

0301-9322/89 $3.00 + 0.00
Pergamon Press/Elsevier

BURNOUT AND DISTRIBUTION OF LIQUID IN EVAPORATIVE CHANNELS OF VARIOUS LENGTHS

V. I. MILASHENKO, B. I. NIGMATULIN, V. V. PETUKHOV and N. I. TRUBKIN
All-Union Scientific Research Institute for Nuclear Power Plants Operation, Moscow, U.S.S.R.

(*Received* 10 *October* 1988; *in revised form* 25 *December* 1988)

Abstract—This paper presents the results of experimental investigations on the distribution of liquid in annular dispersed steam–water upflow in 0.15 and 1.0 m long vertical heated tubes. The effect of heat flux and flow parameters on the distribution of the liquid between the core and the wall liquid film at the end of the heated section and at six points on the 1 m length downstream was investigated. Critical heat flux, liquid film flow rate at burnout and at the onset of annular dispersed flow with subcooled water fed to the heated channel inlet was measured. The rate of total liquid film entrainment relative to the heating is presented.

Key Words: annular flow, burnout, steam–water, experimental data, entrainment, deposition

1. INTRODUCTION

Annular dispersed flow is among the most common flow regimes in two-phase systems. It occurs in a wide range of flow conditions and is characterized by the combined flow of a vapour–droplet core and a wall liquid film with continuous liquid exchange between the two. The rate of liquid film entrainment E and that of core droplet deposition on the film D are of importance. Nevertheless, experimental studies on the hydrodynamics of annular flow in heated pipes are scarce (e.g. Hewitt & Hall-Taylor 1974; Nigmatulin *et al.* 1976a, b; Nigmatulin 1973; Butterworth & Hewitt 1980). Data on burnout (dryout of the liquid film) is much more common and has given rise to a large number of empirical burnout correlations which do not adequately account for all the variables involved. Models which attempt to describe the hydrodynamics of the flow are preferable but the information required by such models is often lacking.

This paper deals with the measurement of the liquid distribution between the core and the wall film, under adiabatic conditions and in the presence of heat flux. In the latter case, critical heat flux and residual liquid film flow rate at the dryout location were recorded. The variation of film flow rate with axial position downstream of the heated section was also investigated, to provide information on the flow relaxation from heat flux-dependent non-equilibrium up to hydrodynamic equilibrium.

2. EXPERIMENTAL ARRANGEMENT

The experiments were conducted on a once-through test rig using high-pressure steam–water flow: for details see figure 1. Two slightly different experimental configurations were used. In one, steam ($P = 140$ b, $T = 420$ °C) and water ($P = 180$ b, $T = 100$°C) were separately metered (at positions 1 in figure 1) and mixed in mixer 2. Downstream of the mixer there is a horizontal stabilizing section, 20 mm i.d.; 3 mm wall thickness, 4 m long ($L/D \sim 200$), followed by a vertical section 13.1 mm i.d., 1.8 m long ($L/D \sim 150$), where equilibrium annular dispersed flow was formed, and a test section with seven wall liquid film samplers, 3–9. The two-phase mixture was cooled and condensed in outlet cooler 10. The test section heated lengths were 0.15 or 1.0 m, and heating was by alternating current.

In the second of the two experimental arrangements, subcooled water was fed to the test section inlet, its flow rate controlled 2 m downstream of the mixer section 2. The other experimental details are the same as for the first setup.

The purpose of the experiments is threefold: firstly, to determine the effect of heat flux on entrainment; secondly, to measure film flow rates at the outlet from the heated section; and thirdly,

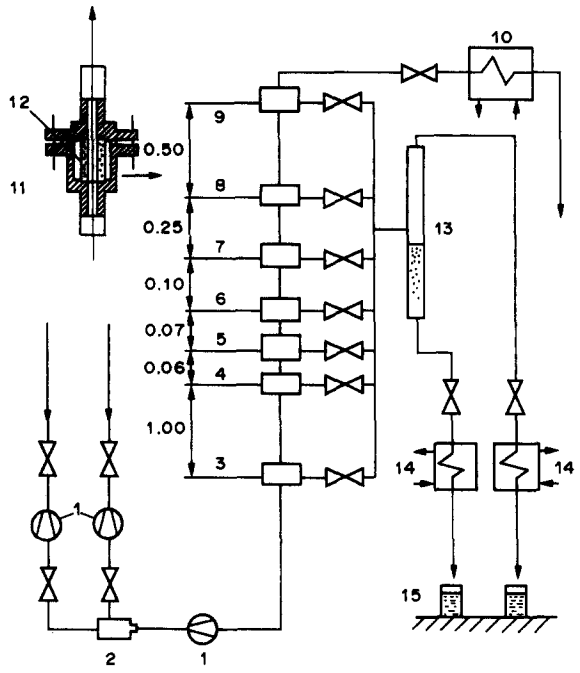

Fig. 1. Test rig: 1, flow meters; 2, mixer; 3–9, film samplers; 10 and 14, coolers; 11, sampling chamber; 12, porous insert; 13, separator; 15, flow rate measurement.

to measure the variation of film flow rate in the unheated section following the heated section. The short, 0.15 m heated section was used for the first of these, while both the 0.15 and 1 m heated sections were used for the second and third measurements.

Liquid film flow rate $\dot{M}_{LF}$ was measured immediately upstream and downstream of the heated section. Downstream of the 0.15 m long heated section five cylindrical inserts 30–44 mm long made of porous nickel (pore size 150 μm, porosity 70%) were located, whose centres from the heated section end were at distances of 0.03, 0.08, 0.15, 0.25 and 0.42 m. Downstream of the 1.0 m long heated section six inserts were provided, also of porous nickel and 50 mm long, at distances from the heated section end of 0.033, 0.089, 0.155, 0.240, 0.5 and 1.0 m.

The measurement technique for liquid film flow rate was analogous to that of Hewitt & Hall-Taylor (1974) and was described in detail by Nigmatulin *et al.* (1976a, b). In sampler 11 the liquid from the film, together with some vapour from the core, was extracted through porous insert 12. The two-phase mixture was separated in separator 13, and flow rates of liquid taken off, $\dot{M}_{LTO}$ and steam condensate taken off $\dot{M}_{GTO}$ were measured by a volumetric technique (see 15 in figure 1). A number (8–10) of mixture flow rates were used to plot the curves in $\dot{M}_{LTO}$ and $\dot{M}_{GTO}$ coordinates. The actual film flow rate $\dot{M}_{LF}$ was obtained by extrapolation of the linear section of $\dot{M}_{LTO} = f(\dot{M}_{GTO})$ to $M_{GTO} = 0$.

Prior to the systematic experiments, liquid film flow rates obtained for various regimes were compared with those of Nigmatulin *et al.* (1976a, b) for adiabatic conditions. The discrepancy was $< 5\%$, which demonstrates both good agreement and equilibrium flow at the given distance from the phase injection location.

During the experiments the following parameters were recorded:

pressure, P	30–100 b
mass flux, $\dot{m}$	1000–3000 kg/m^2 s
heat flux, q	0.15–5 MW/m^2
film flow rate at start of heated section, $\dot{M}_{LFO}$	30, 50, 70 g/s
water subcooling, ΔT_s	3, 10, 35.5, 50°C

The measured parameters were the liquid film flow rates $\dot{M}_{LF}$ downstream of the heated section.

3. RESULTS AND DISCUSSION

3.1. *Effect of heat flux on entrainment*

The differential equations expressing mass conservation for three components of annular dispersed flow—vapour, core droplets and liquid film—within the framework of a one-dimensional steady-state hydrodynamic model in an evaporative channel (Nigmatulin 1973) are as follows:

$$\frac{d\dot{M}'_G}{dz} = \pi d\left(\frac{q}{h_{LG}}\right), \quad [1a]$$

$$\frac{d\dot{M}_{LF}}{dz} = \pi d\left(D - \frac{q}{h_{LG}} - E_d - E_q\right) \quad [1b]$$

and

$$\frac{d\dot{M}_{LE}}{dz} = \pi d(E_d + E_q - D), \quad [1c]$$

where $\dot{M}_G$, $\dot{M}_{LF}$ and $\dot{M}_{LE}$ are the respective flow rates of vapour, liquid film and entrained liquid, a/h_{LG} = rate of film evaporation; E_d = rate of dynamic entrainment from the film surface; E_q = rate of bubble entrainment of the liquid film; and D = rate of core droplet deposition on the film.

Thus, a number of factors influence the liquid film flow rate in a heated channel until the film disappears completely. Of most interest are the rates of bubble entrainment E_q and dynamic entrainment E_d, or total entrainment $E_t = E_q + E_d$.

It has been experimentally shown by Doroschuk & Levitan (1971) that in conditions corresponding to those of the present work steam flowing away from the evaporating film prevents core droplet deposition, and thus $D = 0$.

Integrating the equation of mass conservation for the heated section length L, we obtain:

$$\frac{1}{\pi d}\int_{\text{inlet}}^{\text{outlet}} d\dot{M}_{LF} = \int_0^L \left(D - E_d - E_q - \frac{q}{h_{LG}}\right) dz \quad [2]$$

and so,

$$\frac{1}{\pi d}(\dot{M}_{LG} - \dot{M}_{LFO}) = \left(D - E_d - E_q - \frac{a}{h_{LG}}\right) L; \quad [3]$$

assuming that D, E_d and E_q are constant along the heated section. Since $D = 0$, simultaneous measurement of liquid film flow rates at the beginning and end of the 0.15 m heated section, with different heat flux values, allows the direct total liquid film surface entrainment to be obtained:

$$E_t L = \frac{1}{\pi d}(\dot{M}_{LFO} - \dot{M}_{LF}) - \frac{q}{h_{FG}} L. \quad [4]$$

Note that the length of the heated section was chosen so that quality did not change greatly over its length, but there was sufficient change in $\dot{M}_{LF}$ to give reasonable accuracy.

Analysis of mass transfer mechanisms in evaporative channels with annular dispersed flow enabled us to suppose that the rate of total entrainment E_t depends on the heat flux, pressure, stream velocity in the core U_G and the average liquid film flow rate through the section, $\dot{M}_{LF} = (\dot{M}_{LFO} + \dot{M}_{LF})/2$. The results obtained were plotted as the dimensionless total entrainment $E_t^+ = E_t(\pi d)^2/\dot{M}_{LF}$ against the above flow parameters. Figure 2 shows the effect of the heat flux q on the total entrainment rate. One can see that E_t^+ substantially depends on the heat flux. Treating the data using the least-squares method showed that E_t^+ is proportional to $q^{1.3}$ power, and was extrapolated to the point $E_t^+ = 0, q = 0$.

The total entrainment rate increases substantially with increasing pressure. So, for $q = 3$ MW/m^2 at $P = 50$ b, $E_t^+ \sim 0.07$, while at $P = 100$ b, $E_t^+ \sim 0.28$: a factor of 4 greater. This is thought to be due to greatly decreased surface tension at high pressures.

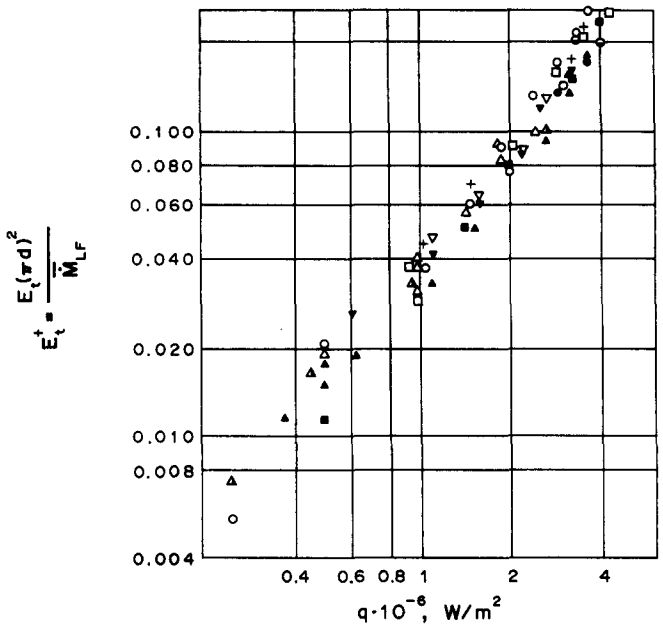

	△	▲	◭	○	●	◒	+	□	●	▽	▼
$\dot{M}_{LFO}$ (g/s)	30	32	30	51	50	49	60	69	72	79	78
U_G (m/s)	19.4	15.8	13.6	13.3	11.5	8.9	7.5	10.5	7.9	7.8	5

Fig. 2. Effect of heat flux on rate of total entrainment for $P = 70$ b.

The experiments showed no marked effect of flow core stream velocity U_G on E_t (figure 2). This is probably because of the relatively small range of velocity variation (at a fixed value of $\dot{M}_{LFO}$), which is insufficient to detect any effect.

In the range of flow parameters studied ($P = 50$ to 100 b, $\dot{m} = 1000$ to 3000 kg/m^2 s, $q = 0.15$ to 4 MW/m^2) the experimental data on the rate of liquid film total entrainment can be correlated within $\pm 20\%$ using the following relationship:

$$E_t^+ = \frac{E_t L \pi d}{\dot{M}_{LF}} = 1.75\left[q \cdot 10^{-6}\left(\frac{\rho_G}{\rho_L}\right)\right]^{1.3}, \qquad [5]$$

where ρ_G and ρ_L are the saturation densities of the steam and water (kg/m^3), respectively, and q is the heat flux (W/m^2). Note that the constant 1.75 has the dimensions of (W/m^2)$^{-1.3}$.

3.2. Film flow rates at the outlet from the heated section

Let us consider the effect of flow conditions on the distribution of liquid in the flow with the 1.0 m heated section. Figure 3 illustrates the effect of inlet liquid subcooling ΔT_s, on $\dot{M}_{LF}/\dot{M}$ as a function of quality. The function is linear and shifts towards increasing quality with increasing ΔT_s. Curve 2 shows the results of Bennett *et al.* (1969) in a tube of 12.6 mm dia and 3.6 m heated section at $\Delta T_s = 34.5$°C. It is seen from comparison with curve 5, plotted for the same conditions but for a heated section of 1.0 m length, that a longer heated section and smaller ΔT_s have similar effects.

Figure 4 shows how the total mass rate $\dot{M}$ influences $\dot{M}_{LF}/\dot{M}$. It is clear that with equal outlet steam qualities x_G, the relative liquid film flow rate $\dot{M}_{LF}/\dot{M}$ substantially decreases with increasing $\dot{M}$ because of increase dynamic and bubble liquid film entrainment.

Comparing data on boundaries of various two-phase flow patterns (see Hewitt & Hall-Taylor 1974; Butterworth & Hewitt 1980; Kirillov *et al.* 1984), and the results obtained within the range of $x_G = 0.5$ to 0.2 (figures 3 and 4) it is possible to obtain the liquid film flow rate $\dot{M}_{LF}/\dot{M}$ or core flow rate $\dot{M}_{LE}/\dot{M}$ at the point of formation of annular dispersed flow. This parameter is very important for two-phase thermal hydraulic calculations. Many investigators assume a condition of 90% and 10% liquid flowing in the film and flow core, respectively, when annular–dispersed

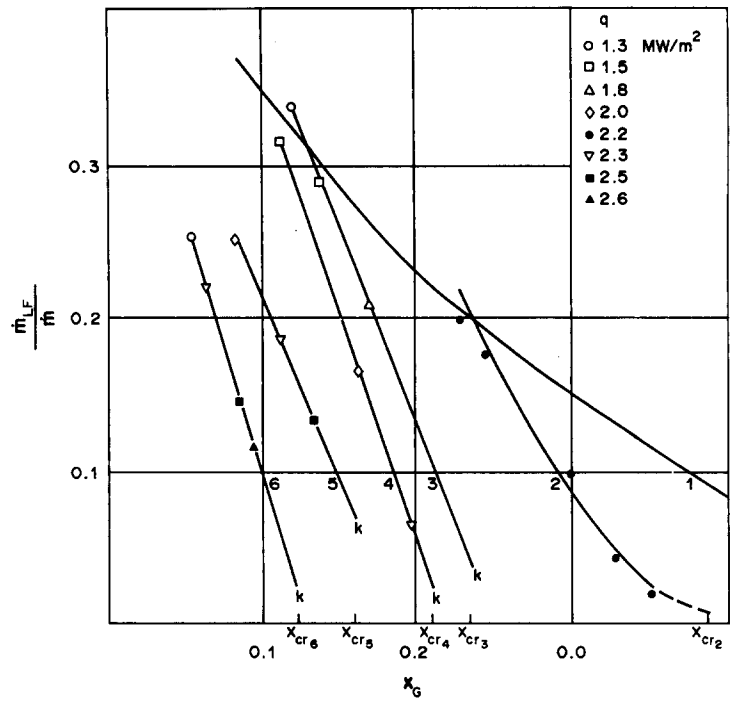

Fig. 3. Effect of subcooling on $\dot{M}_{LF}/\dot{M} = f(x_G)$ for $P = 70$ b and $\dot{m} = 2000$ kg/m² s: 1, equilibrium film flow from Nigmatulin *et al.* (1976a); 2, data of Bennett *et al.* (1969); 3, $\Delta T_s = 3$°C; 4, $\Delta T_s = 10$°C; 5, $\Delta T_s = 34.5$°C; 6, $\Delta T_s = 50$°C.

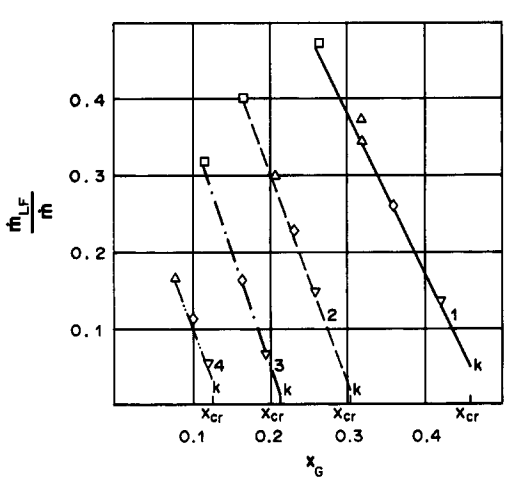

Fig. 4. Effect of mass flux on $\dot{M}_{LF}/\dot{M} = f(x_G)$ for $P = 70$ b and $\Delta T_s = 10$°C: 1, $\dot{m} = 1000$ kg/m² s and $q = 1.5$ MW/m²; 2, $\dot{m} = 1500$ kg/m² s and $q = 1.8$ MW/m²; 3, $\dot{m} = 2000$ kg/m² s and $q = 2.0$ MW/m²; 4, $\dot{m} = 3000$ kg/m² s and $q = 2.3$ MW/m².

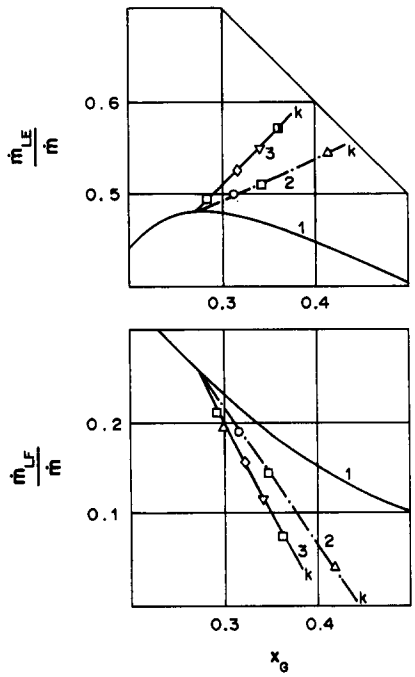

Fig. 5. Effect of heated length on relative liquid film and core flow rates for $P = 70$ b, $\dot{m} = 1500$ kg/m² s, $x_{GO} = 0.28$, $\dot{M}_{LFO}/\dot{M} = 0.245$ and $\dot{M}_{LFO} = 49.6$ g/s: 1, equilibrium data from Nigmatulin *et al.* (1976a); 2, $L_{heat} = 1.0$ m; 3, $L_{heat} = 0.15$ m. Symbols: q (MW/m²) = 0.25 (○), 0.5 (□), 1.0 (△), 2.0 (◇), 3.0 (▽) and 4.0 (◨).

flow occurs. However, for the flow regime with $\dot{m} = 2000\ \text{kg/m}^2\,\text{s}$ and $P = 70$ b, the quality at the onset of annular–dispersed flow, from Kirillov *et al.* (1984), is $x_G \approx 0.05$ and our experimental results give $\dot{M}_{LF}/\dot{M} = 0.25$, so clearly an assumption of 90% liquid in the film would be very inaccurate.

3.3. Film flow rate at the burnout location

There is uncertainty as to whether any liquid film flow exists at the burnout location, and if so, with what flow rate. Because of the lack of data it is commonly assumed that $\dot{M}_{LF}/\dot{M} = 0$ at burnout.

The design of our experimental rig and a specially developed technique allowed determination of $\dot{M}_{LF}/\dot{M}$ for various conditions. In almost all cases a residual liquid film flow rate $\dot{M}_{LFK}$ of approx. 0.02 kg/s (refer to figures 3 and 4, where burnout is designated by the letter "k") for the 1.0 m heated section was recorded. It should be noted that the critical heat flux values of Kirillov *et al.* (1984) agree well with those obtained in this work.

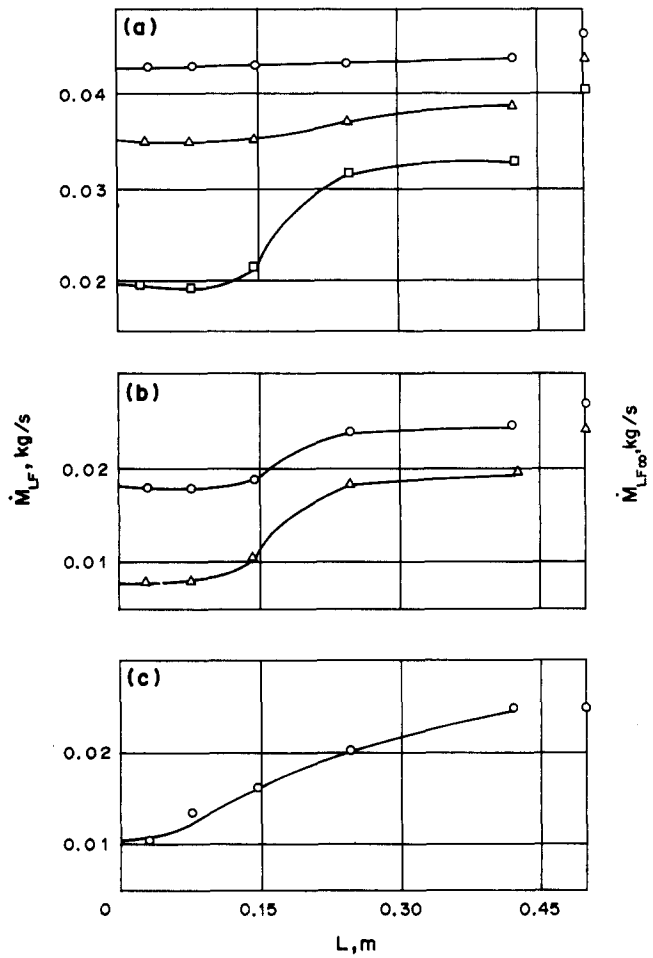

Symbol		$\dot{m}$ (kg/m² s)	x_{GO}	$\dot{M}_{LFO}$	q (MW/m²)	x_G	U_G (m/s)
(a)	○	2000	0.23	0.05	0.5	0.238	10.2
	△	2000	0.23	0.05	1	0.247	10.7
	□	2000	0.23	0.05	2	0.265	14.4
(b)	○	2000	0.3	0.03	1	0.317	13.2
	△	2000	0.3	0.03	2	0.335	13.8
(c)	○	3000	0.31	0.027	2.5	0.333	20.8

Fig. 6. Variation of film flow rate downstream of the heated section for $P = 100$ b and $L_{heat} = 0.15$ m.

The residual liquid film flow rate at the burnout location is due to different mechanisms of wavy film evaporation and destruction, e.g. film dryout in the region between the waves or the breaking down of the film into rivulets and the appearance of dry spots (see Butterworth & Hewitt 1980).

Figure 5 compares the experimental results for different heated lengths with the annular dispersed flow at the inlet for the case $x_{GO} = 0.28$ $\dot{M}_{LFO} = 49.6$ g/s. It is clear that the straight lines 3 and 2 deviate from the equilibrium curve 1 because of the high rate of liquid film entrainment, see particularly the upper part of figure 5. This deviation exists because to obtain the same quality in a short heated section requires a higher heat flux. For example, for $x_G = 0.3$ and $L_{heat} = 0.15$ m, $q = 3$ MW/m^2, while for $L_{heat} = 1.0$ m, $q = 0.5$ MW/m^2.

3.4. Film flow rate variation in the unheated section

To investigate the nature and length of relaxation (restoration of equilibrium annular dispersed flow) the liquid film flow rate ($\dot{M}_{LF}$) was measured at several locations downstream of the heated section. Figures 6–9 illustrate the results for different heated lengths, pressures, mass flow rates and inlet conditions. The right-hand ordinate $\dot{M}_{LF\infty}$ is the equilibrium liquid film flow of Nigmatulin *et al.* (1976a). Figures 6 and 7 show the results for $L_{heat} = 0.15$ m with annular dispersed flow of different qualities fed to the input; the pressures are 100 and 70 b, respectively.

In particular figure 6(a,b) shows the effect of heat flux at fixed $\dot{M}_{LFO}$ [(a) $\dot{M}_{LFO} = 0.05$ kg/s, (b) $\dot{M}_{LFO} = 0.03$ kg/s]. The heat fluxes were 0.5, 1.0 and 2.0 MW/m^2. It is seen in all cases that $\dot{M}_{LFO}$ does not change substantially over the first 0.1 m of the unheated section, which is associated with low entrainment rates (because of low flow core velocities and liquid film flow rates) and low deposition rates (because, according to Doroschuk & Levitan (1971), the steam cross-flow prevents droplet deposition).

According to our estimates, the typical length at which droplets start depositing after heating ceases is 0.1 m. However at $L > 0.1$ m intensive droplet deposition from the oversaturated core is observed. With increasing $\dot{M}_{LF}$, the rate of dynamic entrainment increases and the liquid film flow

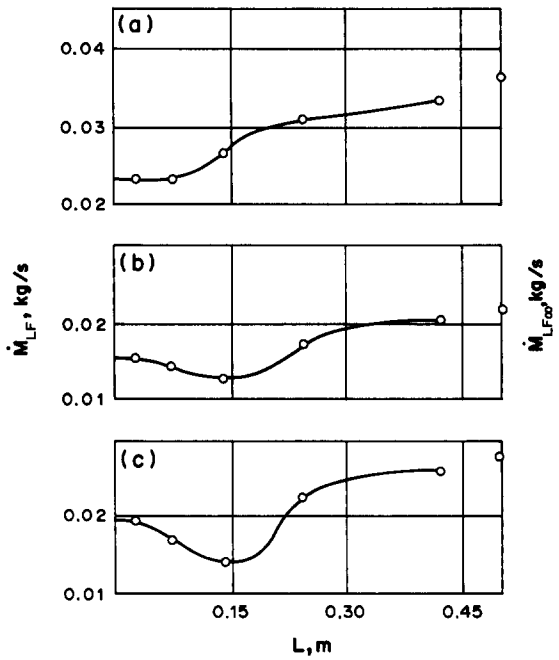

Symbol		$\dot{m}$ (kg/m^2 s)	x_{GO}	$\dot{M}_{LFO}$	q (MW/m^2)	x_G	U_G (m/s)
(a)	○	1500	0.28	0.0495	3	0.342	15.1
(b)	○	2700	0.33	0.028	3	0.361	28.8
(c)	○	3000	0.29	0.327	2	0.31	25.6

Fig. 7. Variation of film flow rate downstream of the heated section for $P = 70$ b and $L_{heat} = 0.15$ m.

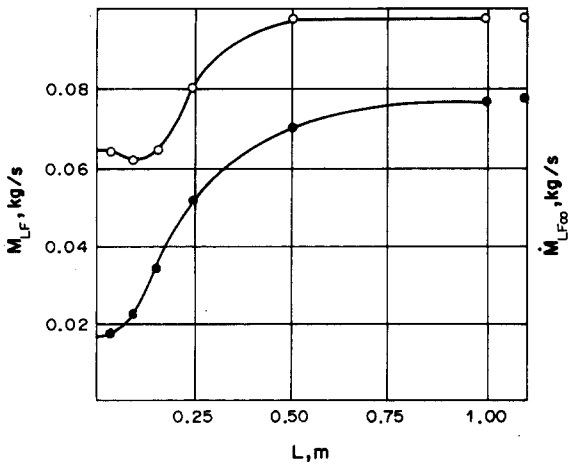

Symbol	P (b)	q (MW/m²)	x_G	U_G (m/s)
○	50	2.8	0.141	16.0
●	70	2.2	0.121	13.7

Fig. 8. Variation of film flow rate downstream of the heated section for $L_{heat} = 1$ m, $\dot{m} = 3000$ kg/m² s and $\Delta T_s = 10$°C.

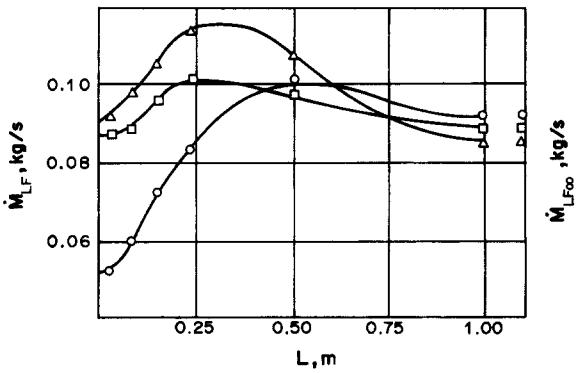

Symbol	ΔT_s (°C)	q (MW/m²)	x_G	U_G (m/s)
□	3	1.3	0.118	8.0
△	10	1.5	0.113	7.7
○	34.5	2.3	0.112	8.0

Fig. 9. Variation of film flow rate downstream of the heated section for $L_{heat} = 1$ m, $\dot{m} = 2000$ kg/m² s and $P = 70$ b.

rate asymptotically approaches the equilibrium value, reaching, at $L = 0.42$ m, values of $\dot{M}_{LF}$ of about (0.8–0.9) $\dot{M}_{LF\infty}$.

An increase in the mass flux up to $\dot{m} = 3000$ kg/m² s [figure 6(c)] results in the disappearance of the region where $\dot{M}_{LF} = \text{const}$. This is due to the increased flow core velocity ($U_G = 20.8$ m/s) and, consequently, the higher rate of deposition [$D \propto U_G$, according to Nigmatulin *et al.* (1981)].

Figure 7(a) shows that the nature of $\dot{M}_{LF} = f(L)$ at 70 b is similar to that at 100 b with the corresponding velocity U_G, while with U_G and $\dot{m}$ increasing [figure 7(b,c)], the nature of relaxation changes. Downstream of the heated section the liquid film flow rate continues to decrease to a minimum at approx. $L = 0.15$ m. This is due to the increasing flow core velocity and, consequently, the rising rate of liquid film entrainment. Here, secondary entrainment due to the depositing droplets may be of importance. It was shown by Guguchkin *et al.* (1985) that under some flow conditions, secondary entrainment may exceed deposition by 20–80%.

Figures 8 and 9 illustrate the variation of the liquid flow rate over the channel length downstream of the 1 m heated section. In this case, the inlet was fed with subcooled liquid with varying degrees of subcooling ΔT_s. In figure 8 the effect of pressure on the flow relaxation is shown. The effects shown in figure 9 are of interest. With increased subcooling and heat flux, different liquid film flow rates were obtained just after the heating section at almost equal values of x_G. It was also found that the liquid film flow rate in the relaxation section can exceed the equilibrium flow rate $\dot{M}_{LF}$. It is evident from both figures that in all cases $\dot{M}_{LF}$ becomes equal to equilibrium $\dot{M}_{LF\infty}$ at approx. $L = 1$ m.

4. CONCLUSIONS

Liquid film flow rates have been measured in steam–water upflow at various pressures in a 13.1 mm dia test section with heated section lengths of 0.15 and 1 m. Measurements were made immediately before and after the heated section, and at various positions in the downstream unheated section. The results show that:

(i) The entrainment rate is strongly dependent on heat flux.
(ii) Film flow rates at dryout are generally greater than zero.
(iii) Droplet deposition is suppressed by vapour generation and this causes a "lag" in the approach to equilibrium in the unheated section.

Acknowledgements—The authors would like to thank Mr A. H. Govan (Harwell) and Dr P. B. Whalley (University of Oxford) for their help in the writing of this paper.

REFERENCES

BENNETT, A. W., HEWITT, G. F., KEARSEY, H. A., KEEYS, R. K. F. & STINCHCOMBE, R. A. 1969 Measurement of liquid film flow rates at 1000 psia in upward steam–water flow in a vertical heated tube. Harwell Report AERE-R5809.

BUTTERWORTH, D. & HEWITT, G. F. 1980 *Two-phase Flow and Heat Transfer* (Russian translation), p. 326. Energy, Moscow.

DOROSCHUK, V. E. & LEVITAN, L. L. 1971 Investigation of droplet deposition from annular dispersed steam–water flow core on wall liquid film. *Therm. Phys. High Temp.* **9,** 591–596.

GUGUCHKIN, V. V., NIGMATULIN, B. I., MARKOVICH, E. E., VASILEV, N. I., ARESTENKO, YU. P. & IVANOVSKAYA, V. I. 1985 Peculiarities in droplet movement and bubbles in wall region. Theses of a report presented at *VII All-Union Conf. on Two Phase Flow in Power Machines and Apparatus*, Leningrad, Vol. 3, pp. 316–317.

HEWITT, G. F. & HALL-TAYLOR, N. S. 1974 *Annular Two-phase Flows* (Russian translation), p. 407. Energy, Moscow.

KAZNOVSKY, S. P., POMET'KO, R. S. & PASHEVICH, V. V. 1978 Burnout and distribution of liquid in annular dispersed flow. *Therm. Phys. High Temp.* **16,** 94–100.

KIRILLOV, P. L., YURIOV, UY. S. & BOBKOV, V. P. 1984 *Handbook on Thermalhydraulics Calculations* (*Nuclear Reactor, Heat Exchangers, Steam Generators*), p. 296. Energoatomizdat, Moscow.

NIGMATULIN, B. I. 1973 Investigation of two-phase annular dispersed flows in heated tubes. *Appl. Mech. tech. Phys.* **4,** 78–88.

NIGMATULIN, B. I., MILASHENKO, V. I. & SHUGAEV, YU. Z. 1976a Distribution of liquid between core and film in annular dispersed steam–water flow. *Teploenergetika* **5,** 77–78.

NIGMATULIN, B. I., MILASHENKO, V. I. & NIKOLAEV, V. E. 1976b Complex investigations of hydrodynamic characteristics of annular dispersed steam–liquid flows. *Therm. Phys. High Temp.* **6,** 1258–1263.

NIGMATULIN, B. I., RACHKOV, V. I. & SHUGAEV, YU. Z. 1981 Investigation of rate of liquid film entrainment in upward steam–water flow. *Teploenergetika* **9,** 63–65.